ELSEVIER

Journal of Power Sources 72 (1998) 178–183

JOURNAL OF POWER SOURCES

The evaluation of $(Ta_{1/2}Cu_{1/2})Sr_2GdCu_2O_{8-\delta}$ as an intercalation cathode material for lithium non-aqueous batteries

W.P. Hagan, R.J. Latham *, W.S. Schlindwein, S.L. Vickers

Solid State Research Centre, School of Applied Sciences, De Montfort University, The Gateway, Leicester, LE1 9BH, UK

Received 19 March 1997; revised 28 August 1997

Abstract

The use of $(Ta_{1/2}Cu_{1/2})Sr_2GdCu_2O_{8-\delta}$ as a cathode caterial for lithium non-aqueous batteries based on a $LiAsF_6$ in propylene carbonate electrolyte is described. Results are presented for the discharge–charge characteristics on cycling. The cell behaviour is discussed in terms of the lithium intercalation process. The effect of chemically prelithiating the materials by a chemical process has been investigated. © 1998 Elsevier Science S.A.

Keywords: Superconductors; Lithium batteries; EXAFS

1. Introduction

Lithium batteries are of considerable commercial interest because of the high ocv and energy density compared with other systems such as alkaline zinc–manganese batteries and the environmentally unfriendly nickel–cadmium battery. The development of rechargeable lithium batteries has been hindered by the passivation of the lithium which limits the cycling characteristics of the battery, while instability may lead to serious safety hazards, especially when caused by abuse or malfunctioning. An alternative approach to the use of a lithium metal anode has been suggested in the concept of the 'rocking chair battery' [1,2]. Here, the anode is a material such as $LiWO_2$ or $LiFe_2O_3$ and the cathode is an intercalation material such as TiS_2, WO_3, NbS_2 or V_2O_5 with a $LiClO_4$ in propylene carbonate electrolyte [3–5]. The concept of the rocking chair battery attracted moderate interest [6,7] until the development of a system based on lithiated carbon and lithium cobalt oxide electrodes [8], but here there are some operational problems associated with the choice of electrolyte and anode material. These latter cells suffer from solvent decomposition on cycling. Thus the development of a stable and safe rocking chair battery requires the replacement of the liquid electrolyte by alternatives which have a wider electrochemical window, especially if this stability is combined with a high ionic conductivity [9].

A number of other approaches have been investigated. Layered two-dimensional structures such as $LiCoO_2$, $LiCo_{1-x}Ni_xO_2$ and $LiNiO_2$ have been evaluated as cathode materials for secondary lithium batteries [10], as well as the three-dimensional tunnel structure associated with $LiMnO_4$ [11,12], and a rechargeable solid state based on a lithium–carbon mix anode, a lithiated manganese dioxide cathode and a polymer electrolyte was recently reported [13] with claims for very little loss of capacity after over 1000 cycles [14]. Another class of materials based on transition metal oxides and which have structures making them possible candidates as intercalation cathodes are the superconductors [15]. In this paper we report the results of investigations using the 1212 phase [16] of $(Ta_{1/2}Cu_{1/2})Sr_2GdCu_2O_{8-\delta}$ in cathode formulations for lithium non-aqueous batteries.

2. Experimental

2.1. Materials

The superconductor was prepared by milling together stoichiometric amounts of Gd_2O_3 (Aldrich), $SrCO_3$ (Fisons), $CuCO_3$ (Fisons) and Ta_2O_5 (BDH). The resulting mixture was fired at 950°C for 12 h and then reground and fired again if necessary until an X-ray powder diffraction

* Corresponding author. School of Applied Sciences, Department of Chemistry, De Montfort University, The Gateway, Leicester, LE1 9BH, England, UK.

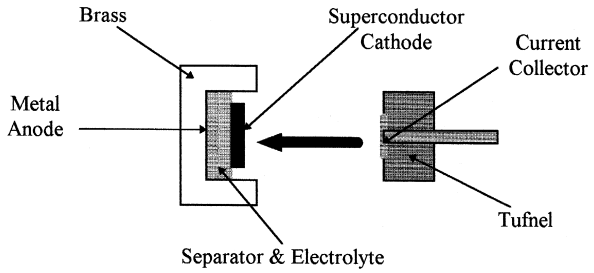

Fig. 1. Cell configuration.

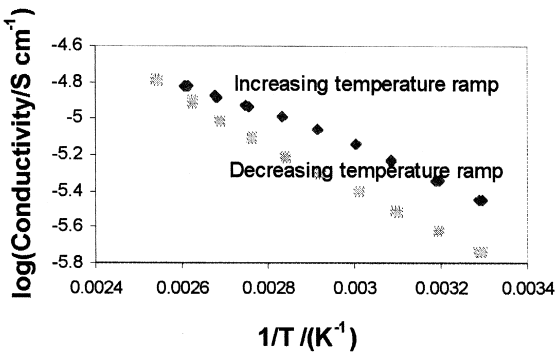

Fig. 3. Conductivity of $(Ta_{1/2}Cu_{1/2})Sr_2GdCu_2O_{8-\delta}$ as a function of temperature.

pattern for the 1212 phase was obtained. The final ceramic material was then mixed with teflon (10% w/w) and graphite (10% w/w) until a consistent texture was achieved. It was then rolled biaxially between PTFE sheets and allowed to air dry to produce thin mechanically stable sheets of about 400 μm thickness. Disks of the formulated cathode material having a mass of about 70 mg were used in the cell construction. The conductivity of a pressed disk of the superconductor material was determined by the AC impedance technique using a Hewlett Packard 4192A Impedance Analyser.

Some cathode formulations were made from samples of the superconductor which had been chemically pretreated using a lithium–naphthalamide lithiating reagent which was prepared by dissolving equimolar quantities of lithium foil and naphthalene in THF at room temperature under an argon atmosphere. Finally, the cathode material was washed with THF to remove any excess lithium naphthalamide reagent.

Electrolyte solutions were prepared by dissolving the required amount of $LiAsF_6$ (Fluka, as received) in propylene carbonate (BDH-HPLC grade, as received).

All materials were opened and all subsequent procedures were carried out under a dry argon atmosphere ($<$ 50 ppm water) in a high integrity glove box.

2.2. Cell tests

Fig. 1 shows the air tight test cell in which the non-aqueous $LiAsF_6$ electrolyte was supported on a paper separator between the lithium foil anode and the cathode formulation described above. The performance of the cells was monitored using a computer interface battery test unit (H&L Battery Testing Unit Type 02B). Test cells were typically discharged at 25 μA cm^{-2} and charged at 12.5 μA cm^{-2}. A cell was deemed to have failed when its voltage had decayed to 0.5 V.

2.3. EXAFS

The EXAFS technique was used to explore the local structure for samples before and after chemical lithiation. The copper K-edge and the tantalum L_{III}-edge were examined on Station 7.1 of the SRS at CCLRC Daresbury Laboratory. The beam energy was 2 GeV and the stored ring current was 150–200 mA. Data analysis was performed using the suite of EXAFS programs available at Daresbury Laboratory.

3. Results and discussion

Fig. 2 shows the initial discharge curve for a typical cell at 25°C. There is an initial polarisation and the voltage rapidly falls from about 2.5 V to 1.8 V when the load is applied. The voltage continues to fall to about 1.2 V and

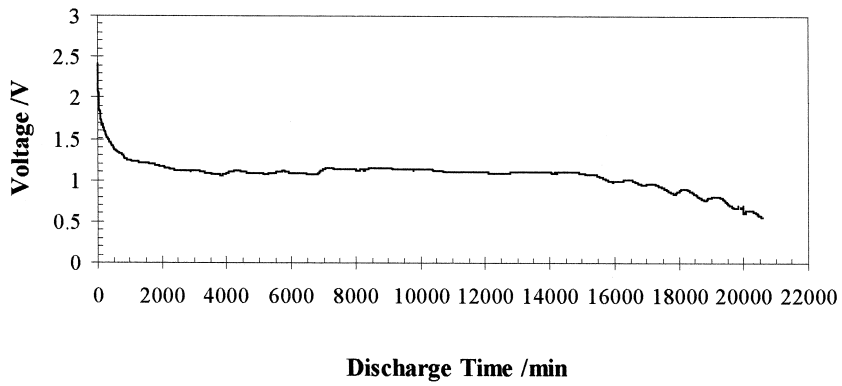

Fig. 2. Li/$LiAsF_6$ in PC/$(Ta_{1/2}Cu_{1/2})Sr_2GdCu_2O_{8-\delta}$ discharged at 25 μA cm^{-2} at 298 K.

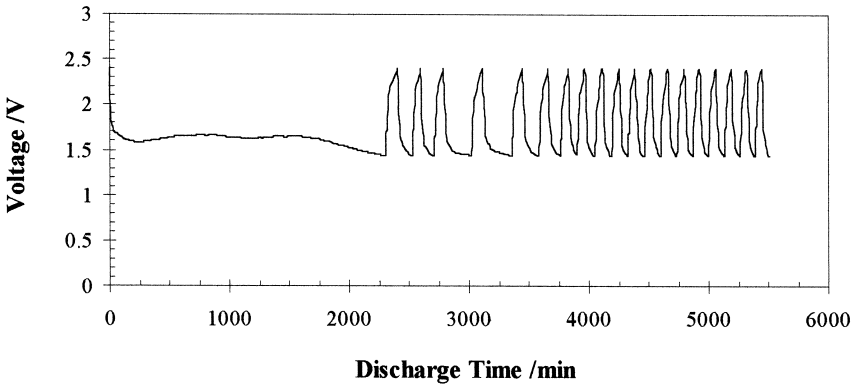

Fig. 4. Li/$LiAsF_6$ in PC/$(Ta_{1/2}Cu_{1/2})Sr_2GdCu_2O_{8-\delta}$ discharged at 25 μA cm^{-2} to 1.5 V and then charged at 12.5 μA cm^{-2} at 298 K.

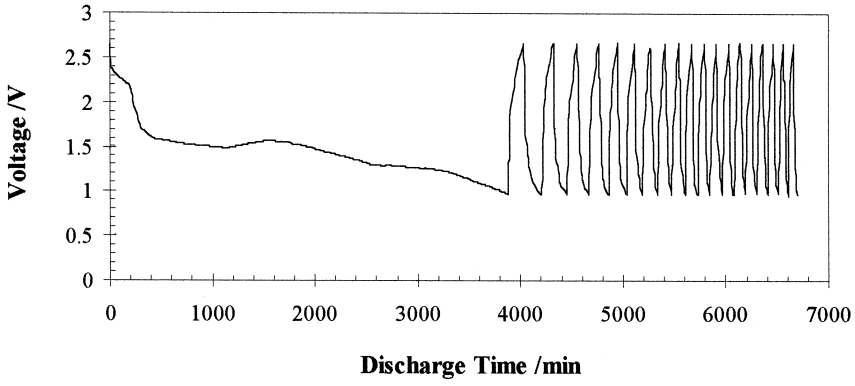

Fig. 5. Li/$LiAsF_6$ in PC/$(Ta_{1/2}Cu_{1/2})Sr_2GdCu_2O_{8-\delta}$ discharged at 25 μA cm^{-2} to 1.0 V and then charged at 12.5 μA cm^{-2} at 298 K.

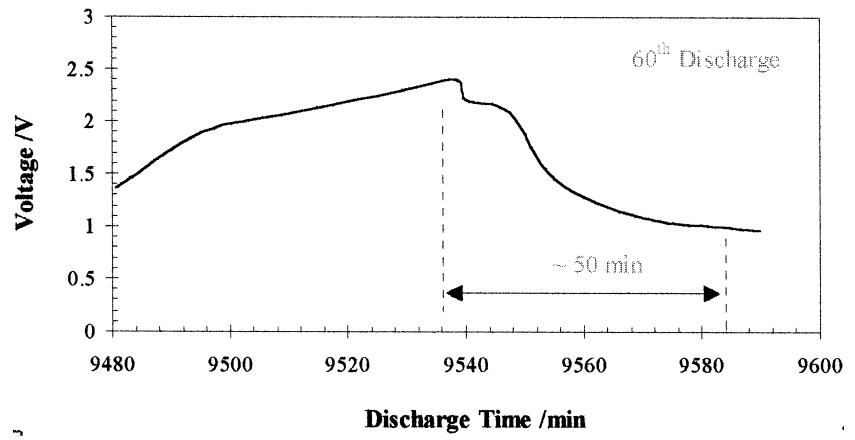

Fig. 6. The 60th cycle for a cell discharged at 25 μA cm^{-2} to 1.0 V and then charged at 12.5 μA cm^{-2} at 298 K.

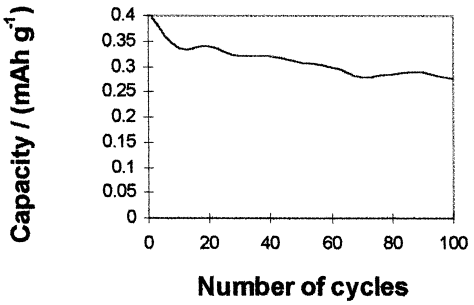

Fig. 7. The effect of cycling on cell capacity after the first discharge process.

the discharge curve then has a characteristic plateau until the cells polarise rapidly after ~16 000 min until the onset of failure at ~20 000 min. The initial polarisation response indicates a cell capacity of ~30 C cm^{-2}. These current densities may appear to be low for a system based on a liquid electrolyte but this is probably due to the room temperature conductivity of the superconductor (~ 10^{-5} S cm^{-1}). A plot of the conductivity of the superconductor as a function of temperature is shown in Fig. 3.

The discharge characteristics were found to be different after the first 1–2 cycles and this was investigated by following two different cycling regimes. Fig. 4 shows the effect of discharging to 1.5 V at 25 μA cm^{-2} before charging to 2.5 V at 12.5 μA cm^{-2} and then repeating the cycle. Fig. 5 illustrates the behaviour when a cell is discharged to 1.0 V and then cycled at the same rates of discharge and charge. A cycle life of up to 100 cycles was observed with initial cycles having a discharge time of ~60 min (~0.35 mA h g^{-1} of cathode material) and that for the 60th cycle, for example, decaying to ~50 min (~0.3 mA h g^{-1} cathode material). Fig. 6 shows a typical discharge curve for the 60th discharge cycle of a cell discharged to 1.0 V. Although the cells could be processed through 100 cycles, optimisation is required because the cycled charge is less than 1% of the initial cell capacity of ~120 mA h g^{-1} cathode material. This can be seen in Fig. 7 which shows how the cell capacity changes on cycling after the end of the first cycle during which there is a substantial loss in capacity.

As expected, the initial discharge time for cells discharged to 1.0 V is longer than for those discharged to only 1.5 V. On first inspection the results shown in Figs. 4 and 5 may appear to be similar in that at some stage of the cell discharge (~2500 min in Fig. 4 and ~4000 min in Fig. 5), the charge–discharge cycles to an upper limit of 2.5 V are commenced. In both cases, there is a loss of capacity and this is commensurate with an irreversible process. When the cells are discharged to 1.5 V the capacity is not completely exhausted and the presence of the irreversible reaction is indicated by the enhanced capacity between cycles 4 and 20 as shown in Fig. 8. Discharge to 1 V results in a more rapid loss of capacity. A possible interpretation for the observation that the first cycle is different from the subsequent cycles is that the intercalation of lithium from the electrolyte into the cathode takes place in three stages. On cycling there is then partial depletion of the intercalated lithium from the cathode and for all following cycles the behaviour is the same. As shown in Fig. 5, the initial discharge curve has three characteristic regions at ~2.3, 1.5 and 1.4 V which suggest that the lithium insertion into the cathode during battery discharge is not by a simple mechanism. This is consistent with the results from cyclic voltammetry experiments on these cathode materials which are reported elsewhere [17]. These show multiple peaks on both cathodic and anodic scans which can be attributed to the insertion and extraction of lithium. The magnitude of first peak on the cathodic scan at about 1.38 V decreases significantly as the number of scans increases and this confirms the observation that the discharge times reported here are constant after the first cycle and do not depend on the depth of discharge. Since depth of discharge depends not only on the cut off potential but also on the rate of discharge further experiments to explore these effects were carried out and Fig. 9 shows the cell capacity as a function of

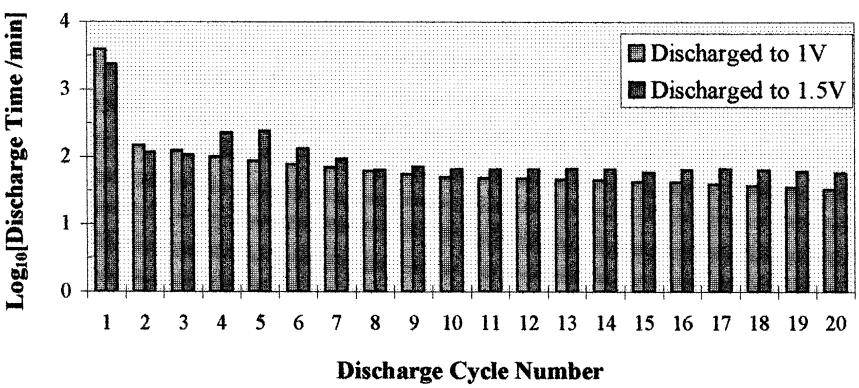

Fig. 8. Comparison of discharge time and cycle number for cell cycles shown in Fig. 4Fig. 5.

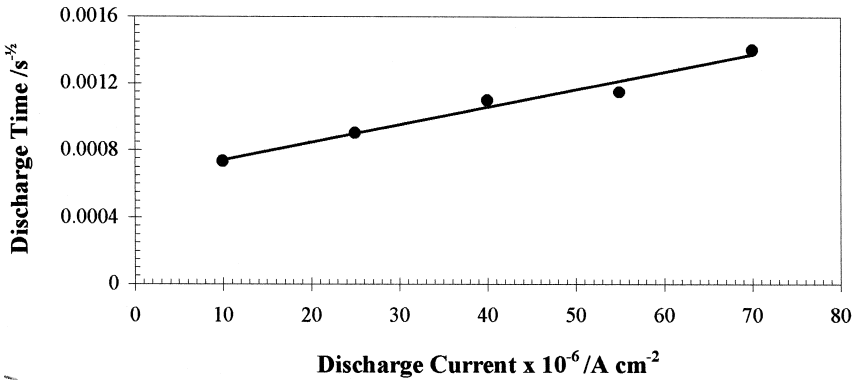

Fig. 9. Discharge time as a function of discharge current.

discharge current for the first discharge process to a cut off potential of 1 V. The effect of lithium insertion was tested by chemical prelithiation of cathode samples. After prelithiation the discharge time for the first cycle is no longer than those of the subsequent cycles and this is in agreement with the cyclic voltammetry results where the first cathodic peak is absent.

The effect of prelithiation was also investigated by use of the EXAFS technique. Fig. 10 shows the results for the Fourier transform of the EXAFS spectrum for the copper K-edge of the cathode material before and after chemical prelithiation. Fig. 11 shows the results of the tantalum L_{III}-edge EXAFS experiments on the same samples. The experimental EXAFS spectra associated with the copper K-edge and the tantalum L_{III} edge in the samples before and after chemical lithiation are very similar and there is no change in the interatomic distances obtained from the peaks of the Fourier transforms of these spectra. Inspection reveals a significant reduction in the amplitude of the Cu–O peak at ≈ 2.0 Å after the chemical lithiation process. This is surprising because EXAFS studies of the cation environments in $Ba_2YCu_3O_7$ by Gurman et al. [18] suggested that the Cu–O bond in those types of superconductor material was very rigid on the basis that a comparison of the results at room temperature and 77 K revealed only a small reduction in the amplitude of the Cu–O peak compared to those of the Ba–O and Y–O peaks. The EXAFS results reported here relate to the chemical insertion of lithium into the cathode lattice and although a change in the copper–oxygen coordination number is not expected, some local structural perturbations may occur as the lithium is introduced.

When lithium is inserted into the stable 1212 phase of these materials, which have layered perovskite lattices, it is possible that the preferred perovskite structural environment for the copper is distorted. The initial discharge process may be associated with deep and irreversible intercalation of lithium into the host lattice and this leads to the greatly reduced capacities on subsequent cell cycles. It is possible that there is a gradual transformation of the original lattice as a result of some chemical bonding with the intercalated lithium. When this process is complete,

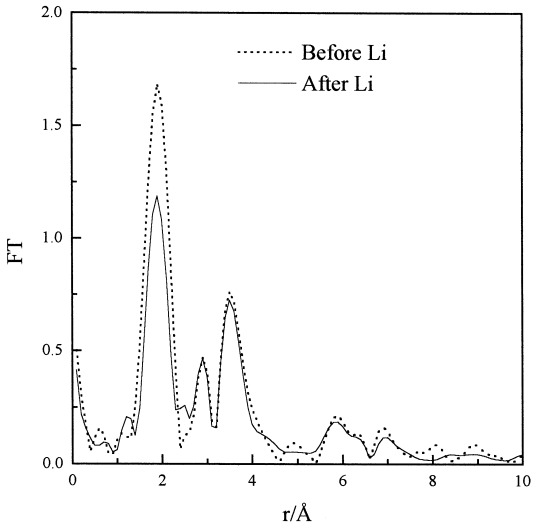

Fig. 10. Fourier transform of the copper K-edge EXAFS spectrum before and after chemical lithiation of the cathode material.

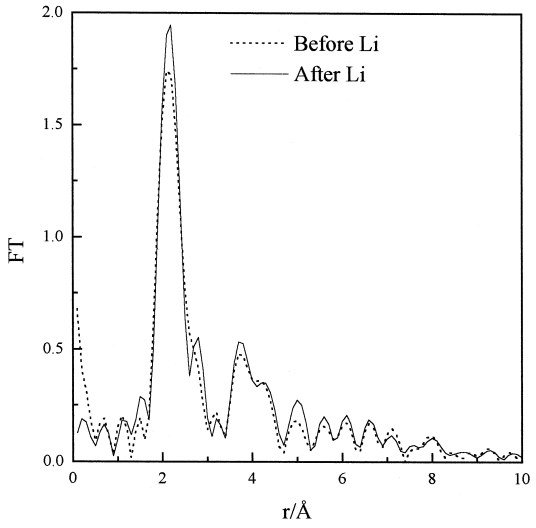

Fig. 11. Fourier transform of the tantalum L_{III}-edge EXAFS spectrum before and after chemical lithiation of the cathode material.

subsequent cycling behaviour is confined to non-bound lithium and the cell may be cycled more than 100 times.

4. Conclusions

Preliminary investigations suggest that superconductors containing transition metal oxides may be used as a component in the formulation of intercalation cathodes for use in lithium non-aqueous battery systems. The cell performance is characterised by:

- Good open circuit voltage ($\sim$ 3 V),
- Although the cells may be cycled up to 100 times, optimisation is required because the cycled charge is less than 1% of the cell capacity,
- Different characteristics for the first one or two cycles.

References

[1] B. Scrosati, J. Electrochem. Soc. 139 (1992) 2776.
[2] M. Armand, Materials for advanced batteries, in: D.W. Murphy, J. Broodhead, B.C.H. Steele (Eds.), Plenum, New York, 1980, p. 145.
[3] M. Lazzari, B. Scrosati, J. Electrochem. Soc. 127 (1980) 773.
[4] B. DiPietro, M. Patricia, B. Scrosati, J. Power Sources 8 (1982) 289.
[5] M. Lazzari, B. Scrosati, US Patent 4464447, 1984.
[6] J. J Auborn, Y.L. Barberio, J. Electrochem. Soc. 134 (1987) 638.
[7] K.W. Semkov, A.F. Sammels, J. Electrochem. Soc. 134 (1987) 766.
[8] T. Nagaura, K. Tazawa, Prog. Batteries Sol. Cells 9 (1990) 20.
[9] F. Croce, S. Passerini, B. Scrosati, J. Electrochem. Soc. 141 (1994) 1405.
[10] K. Mizushima, P.C. Jones, P.C. Wiseman, J.B. Goodenough, Mater. Res. Bull. 15 (1980) 783.
[11] M.M. Thackeray, W.I.F. David, P.G. Bruce, J.B. Goodenough, Mater. Res. Bull. 18 (1983) 461.
[12] A. Yamada, K. Miura, K. Hinokuma, M. Tanaka, J. Electrochem. Soc. 142 (1995) 2149.
[13] C.E. Newham, N. Scholey, K. Green, 19th International Power Sources Symposium, 1995, p. 285.
[14] A. Coghlan, New Scientist, April 1995, 25.
[15] A. Schauwers, Elekronica 42 (1994) 16.
[16] Y. Xin, Z.Z. Sheng, D.X. Gu, D.O. Pederson, Physica C 177 (1991) 183.
[17] W.P. Hagan, S.L. Vickers, C. Capiglia, J. Power Sources 65 (1997) 235.
[18] S.J. Gurman, G. Diakun, B. Dobson, S. Abell, G.N. Greaves, R. Jordan, J. Phys. C 21 (1988) L475.